JOURNAL OF Materials CHEMISTRY

Synthesis and characterization of new layered mixed metal phosphonate materials magnesium–zinc phosphonates $Mg_{1-x}Zn_x(O_3PR)\cdot H_2O$ and nickel–zinc phosphonates $Ni_{1-x}Zn_x(O_3PR)\cdot H_2O$ using mixed divalent magnesium–zinc and nickel–zinc hydroxides

Bouzid Menaa and Ian J. Shannon*

School of Chemical Sciences, University of Birmingham, Birmingham, UK B15 2TT. E-mail: I.Shannon@bham.ac.uk

Received 26th June 2001, Accepted 25th October 2001
First published as an Advance Article on the web 18th December 2001

Layered mixed divalent metal phosphonates $Mg_{1-x}Zn_x(O_3PR)\cdot H_2O$ [with R = CH_3, C_2H_3, C_6H_5] and $Ni_{1-x}Zn_x(O_3PR)\cdot H_2O$ [with R = CH_3, C_2H_3, C_6H_5, $(CH_2)_2COOH$] have been prepared by heating, respectively, mixed divalent magnesium–zinc hydroxides and nickel–zinc hydroxides above the melting point of the phosphonic acid being used. A range of pre-formed mixed divalent metal hydroxides $Mg_{1-x}Zn_x(OH)_2$ and $Ni_{1-x}Zn_x(OH)_2$ with different ratios of Zn content (x = 0, 0.1, 0.25, 0.5) are obtained by isomorphous substitution of zinc into the, respective, $Mg(OH)_2$ and $Ni(OH)_2$ brucite-type structure: space group $P\bar{3}m1$; a = 3.13–3.15 Å, c = 4.63–4.77 Å). The phosphonate materials have been characterized by X-ray powder diffraction, IR, TGA, and ^{31}P MAS NMR. $Mg_{1-x}Zn_x(O_3PR)\cdot H_2O$ and $Ni_{1-x}Zn_x(O_3PR)\cdot H_2O$ crystallize in an orthorhombic system with space group $Pmn2_1$ with b = 5.55–5.69 Å, c = 4.71–4.86 Å and a varying according to the size of the organic group R.

Introduction

Studies of layered metal phosphonate materials, $M(O_3PR)_x\cdot yH_2O$, represent an important step in the development of inorganic–organic hybrid compounds.[1] Since the early work on zirconium[2–4] and the isomorphous titanium phosphates, the study has been extended to phosphonates of these tetravalent metals.[5,6] The majority of works in the area have seen an increasing interest in the preparation of derivatives of transition-metal phosphonates and many investigations have been reported about the synthesis, crystal structures, and properties of divalent metal (*e.g.*, Mg, Zn, Ni, Co, Mn, Cu, Cd)[7–13] and trivalent metal phosphonates (*e.g.*, Mn, Al).[14–16]

These compounds may be synthesized by a range of different methods: by hydrothermal methods, by co-precipitation[7,12,16] from a solution of the appropriate salt with the required phosphonic acid under controlled pH condition, or more recently by using soluble organometallic precursors for the synthesis of zinc phosphonates.[17]

The structure[7–9] of M^{II} phosphonates, $M^{II}(O_3PR)\cdot H_2O$, differs greatly from that observed for the M^{IV} phosphonates[18] of general formula $M^{IV}(O_3PR)_2$. For the latter (such as α-Zr phosphonates) the octahedral coordination sphere around each metal centre is built up from six separate phosphonate groups. Contrastingly, in the M^{II} systems (which contain half as many phosphonate groups) two of the oxygen atoms chelate a single metal centre and also bridge across to an adjacent metal cation, rendering a water molecule necessary to complete the coordination sphere. The structural aspects of layered divalent metal phosphonates have been well described in the literature. Cunningham *et al.*[19] reported the synthesis of divalent metal phosphonates $M^{II}(O_3PR)\cdot H_2O$ (M = Mg, Mn, Co, Ni) and demonstrated that the metal coordination was approximately octahedral in all from consideration of electronic spectra. Martin *et al.*[9] and Cao *et al.*[8] reported that Ni, Mg, Zn, Mn phenylphosphonates were isostructural crystallizing in an orthorhombic unit cell, space group: $Pmn2_1$, with a = 5.61–5.74, b = 14.28–14.45 and c = 4.78–4.82 Å. However, the structure of Cu^{II} phosphonate materials differs from their analogues, as they contain five-coordinate copper atoms.[11,12]

Most of the studies concerning phosphonate materials have been carried out with different organic groups, *e.g.* alkyl, aryl, and functional groups such as amino groups, $-NH_2$, and carboxylic acids, –COOH.[20–22] The large choice of metals that can be used to form the inorganic backbone, together with the range of organic groups that may be attached, gives a great variety of functionality to these compounds, and has led to considerable interest in building microporosity into the structure.[23,24] Also, the compounds containing acidic groups, such as sulfonic acids, $-SO_3H$,[25–28] or carboxylic acids, –COOH,[29] in which their mobile proton can readily diffuse along the layers, make them suitable for use as proton conductors, catalysts,[30] and as cation exchangers.[5] Intercalation reactions, for instance with alkylamines, of the divalent metal phosphonates[10,31–36] gives these materials potential applications as sorbents.

Most of the studies to date have concentrated on systems in which there is only one type of metal present within the layered phosphonate materials. In this work, we have expanded the studies to systems containing two metals within the metal phosphonate layers in which both are divalent. We have prepared a series of divalent mixed magnesium–zinc phosphonates $Mg_{1-x}Zn_x(O_3PR)\cdot H_2O$ and nickel−zinc phosphonates $Ni_{1-x}Zn_x(O_3PR)\cdot H_2O$ with different organic groups attached to the inorganic backbones, to form layered mixed divalent metal phosphonates which have similar structure to those compounds containing only one metal. Materials, such as those prepared here containing two different metals in the same valence state, could enable the tuning of the adsorption, ion exchange and proton conduction properties, and have further potential for modification to generate much sought after

 DOI: 10.1039/b105559n

regular porous structures on account of differing exchange properties at each metal site.

Previous attempts to synthesize mixed metal phosphonates, by methods similar to the conventional solution based method described above, generally result in the formation of a mixture of the two individual metal phosphonates. Bujoli and co-workers,[37] however, did successfully obtain a mixed Zn^{II}–Mn^{II} phosphonate in which the zinc atoms have tetrahedral coordination while the manganese atoms are octahedrally coordinated.

Hix and Harris[38] demonstrated that nickel phosphonates could be prepared by heating a mixture of the desired phosphonic acid and pre-formed $Ni(OH)_2$ in a sealed vessel above the melting point of the phosphonic acid being used. This method provided us with a general route to prepare the mixed divalent metal phosphonate materials using a range of mixed divalent metal hydroxide precursors $Mg_{1-x}Zn_x(OH)_2$ and $Ni_{1-x}Zn_x(OH)_2$ (with $x = 0$, 0.1, 0.25, 0.5) obtained by isomorphous substitution of zinc into the respective $Mg(OH)_2$ and $Ni(OH)_2$ brucite-type structure.

In this paper, we focus on the structural characterization of $Mg_{1-x}Zn_x(O_3PR)\cdot H_2O$ and $Ni_{1-x}Zn_x(O_3PR)\cdot H_2O$, where both have same layered structure as $M^{II}(O_3PR)\cdot H_2O$ and for which both metals are octahedrally coordinated.

Experimental

Starting materials

Chemicals were from commercial sources. Zinc nitrate hexahydrate and nickel nitrate hexahydrate obtained from Avocado, and magnesium nitrate hexahydrate and the different phosphonic acids (methylphosphonic acid, vinylphosphonic acid, phenylphosphonic acid and 2-carboxyethyl phosphonic acid) obtained from Aldrich, were used without further purification.

Characterization

Powder X-ray diffraction data were recorded using Cu-Kα_1 radiation ($\lambda = 1.54056$ Å) on a Siemens D5000 or Stoe Stadi-P diffractometer operating in transmission mode. Indexing of the data were carried out using the packaged programs.

FTIR spectra were recorded as KBr pellets using a Perkin Elmer Paragon 1000 FTIR spectrometer.

Thermogravimetric analysis was carried out using either a TA instruments SDT2960 simultaneous DTA–TGA thermogravimetric analyser or a Stanton Redcroft 870 instrument. Samples, referenced against recalcined alumina, were heated in air with a rate of 10 °C min^{-1} from 25 °C to a maximum of 1000 °C in an atmosphere of flowing oxygen (110 ml min^{-1}).

Solid state ^{31}P MAS NMR spectra were recorded using Chemagnetics CMX Infinity 300 spectrometer with a 3.2 mm double resonance probe or a 4 mm resonance probe. The standard cross polarisation pulse sequence was used with a contact time of 6.0 ms and a recycle delay of, typically 15.0 s, a spinning frequency of 7 kHz ± 2 Hz and a ^1H decoupling field strength of *ca.* 100 kHz. The spectra are referenced to phosphoric acid (85% per weight) at 0 ppm.

Preparation of magnesium–zinc hydroxide and nickel–zinc hydroxides precursors

The range of magnesium–zinc hydroxides $Mg_{1-x}Zn_x(OH)_2$ with different ratios of zinc content ($x = Zn/(Mg + Zn) = 0$, 0.1, 0.25, 0.5) were prepared using the following standard procedure: 75 ml of a 0.04 M (in metal) solution, containing magnesium nitrate hexahydrate $Mg(NO_3)_2\cdot 6H_2O$ and zinc nitrate hexahydrate $Zn(NO_3)_2\cdot 6H_2O$ to give the desired Mg : Zn ratio, in distilled water was slowly dropped into 75 ml of 0.4 M sodium hydroxide solution with stirring to obtain a gel of stoichiometry $Mg_{1-x}Zn_x(NO_3)_2$: 10 NaOH : 210 H_2O.

Upon complete addition, the mixture was refluxed for 6 hours. The white precipitate formed was then filtered off, washed with distilled water until pH neutral and dried in the oven at 60 °C.

Nickel–zinc hydroxides were obtained by the same procedure, replacing $Ni(NO_3)_2\cdot 6H_2O$ for $Mg(NO_3)_2\cdot 6H_2O$ in the synthesis.

Preparation of magnesium–zinc phosphonate and nickel–zinc phosphonate materials

Samples of $Mg_{1-x}Zn_x(O_3PR)\cdot H_2O$ were prepared by mixing the pre-formed magnesium-zinc hydroxides $Mg_{1-x}Zn_x(OH)_2$ (1 equiv.) with a stoichiometric quantity of the relevant phosphonic acid H_2PO_3R (R = Ph or Me, 1 equiv.). To obtain the corresponding magnesium–zinc vinylphosphonates, however, an excess of vinylphosphonic acid (1.2 equiv.) was used. The mixtures were ground, placed in autoclaves, and heated above the melting point of the phosphonic acid (Table 1) for 3 days, before the resulting products were washed with deionised water to remove any unreacted phosphonic acid and recovered by filtration. The resulting solid products were then dried in the oven at 60 °C.

$Ni_{1-x}Zn_x(O_3PR)\cdot H_2O$ were prepared by the same procedure and conditions, instead using the corresponding nickel–zinc hydroxides. For the preparation of nickel–zinc 2-carboxyethylphosphonates a stoichiometric ratio of $Ni_{1-x}Zn_x(OH)_2$ to 2-carboxyethylphosphonic acid was used.

The elemental analyses for C and H and thermogravimetric analysis data are in good agreement with the proposed formulations as shown below for the series $Mg_{1-x}Zn_x(O_3PC_6H_5)\cdot H_2O$. Representative data are also given for a selection of other materials prepared.

$Mg(O_3PC_6H_5)\cdot H_2O$. Anal. Calc. for $C_6H_7O_4PMg$ (M = 198.4 g mol^{-1}): C, 36.32; H, 3.53. Found: C, 36.32; H, 3.67%. TGA (water loss): calc, 9.07; found, 9.25%.

$Mg_{0.9}Zn_{0.1}(O_3PC_6H_5)\cdot H_2O$. Anal. Calc. for $C_6H_7O_4PMg_{0.9}Zn_{0.1}$ (M = 202.32 g mol^{-1}): C, 35.59; H, 3.46. Found: C, 35.49; H, 3.38%. TGA (water loss): calc, 8.89; found, 8.95%.

$Mg_{0.75}Zn_{0.25}(O_3PC_6H_5)\cdot H_2O$. Anal. Calc. for $C_6H_7O_4PMg_{0.75}Zn_{0.25}$ (M = 208.67 g mol^{-1}): C, 34.53; H, 3.35. Found: C, 34.30; H, 3.40%. TGA (water loss): calc, 8.62; found, 8.85%.

$Mg_{0.5}Zn_{0.5}(O_3PC_6H_5)\cdot H_2O$. Anal. Calc. for $C_6H_7O_4PMg_{0.5}Zn_{0.5}$ (M = 218.93 g mol^{-1}): C, 32.91; H, 3.22. Found: C, 32.90; H, 3.18%. TGA (water loss): calc, 8.22; found, 8.17%.

$Zn(O_3PC_6H_5)\cdot H_2O$. Anal. Calc. for $C_6H_7O_4PZn$ (M = 239.48 g mol^{-1}): C, 30.09; H, 2.92. Found: C, 30.16; H, 3.00%. TGA (water loss): calc, 7.52; found, 7.65%.

$Mg_{0.75}Zn_{0.25}(O_3PCH_3)\cdot H_2O$. Anal. Calc. for $CH_5O_4PMg_{0.75}Zn_{0.25}$ (M = 146.59 g mol^{-1}): C, 8.19; H, 3.41. Found: C, 8.35; H, 3.64%. TGA (water loss): calc, 12.28; found, 12.35%.

$Mg_{0.75}Zn_{0.25}(O_3PC_2H_3)\cdot H_2O$. Anal. Calc. for $C_2H_5O_4PMg_{0.75}Zn_{0.25}$ (M = 158.61 g mol^{-1}): C, 15.14; H, 3.17.

Table 1 Melting points of the different phosphonic acids used and the temperature at which heating was carried out in the preparation of mixed divalent magnesium–zinc and nickel–zinc phosphonate materials

Phosphonic acid	Melting point/°C	Heating point/°C
Methyl	104–105	145
Vinyl	41–45	90
Phenyl	163–166	190
2-Carboxyethyl	164–165	190

Found: C, 15.04; H, 3.17%. TGA (water loss): calc, 11.35; found, 11.80%.

$Ni_{0.5}Zn_{0.5}(O_3P(CH_2)_2COOH)\cdot H_2O$. Anal. Calc. for $C_3H_7O_6PNi_{0.5}Zn_{0.5}$ (M = 232.1 g mol^{-1}): C, 15.53; H, 3.01. Found: C, 15.62; H, 3.22%. TGA (water loss): calc, 7.75; found, 8.15%.

Results and discussion

Mixed divalent metal hydroxides

The pre-formed $Mg_{1-x}Zn_x(OH)_2$ powders were all white, while the $Ni_{1-x}Zn_x(OH)_2$ samples were green in colour becoming more pale as the Zn content increased.

The powder X-ray diffraction patterns (Fig. 1 and Fig. 2) recorded at ambient temperature for the mixed divalent magnesium–zinc and nickel–zinc hydroxides show that the zinc cations, Zn^{2+}, isomorphously replace Mg^{2+} and Ni^{2+}, respectively, into the brucite structures of $Mg(OH)_2$ and $Ni(OH)_2$ for a range of Zn/(Mg + Zn) and Zn/(Ni + Zn) ratios x = 0, 0.1, 0.25, 0.5. All these samples crystallized with the brucite-type structure, space group $P\bar{3}m1$ and with similar cell parameters $a = b$ = 3.13–3.15, c = 4.63–4.77 Å. Attempts to prepare pure $Zn(OH)_2$ (x = 1) using the same reaction conditions were unsuccessful, as we obtain instead zinc oxide, ZnO, as confirmed by powder X-ray diffraction. It has also not yet been possible to find appropriate conditions in order to obtain single phase mixed divalent metal hydroxides for high contents of zinc within the structure. In fact for $x > 0.5$ and for $x \neq 1$, we obtain a mixture of two different phases composed of a brucite-like structure of M–Zn hydroxides (with M = Mg, Zn) and the pure ZnO.

We can see from Table 2 and Table 3 than the a cell parameter increases with increasing Zn content into $Mg_{1-x}Zn_x(OH)_2$ due to the influence of the higher ionic radius of Zn^{II} than Mg^{II}. For the same reason the increase of a structural parameter in $Ni_{1-x}Zn_x(OH)_2$ is not as significant. Contrastingly, we observe a slight decrease in the c parameter for both series of hydroxides, due to stronger interactions between the layers.

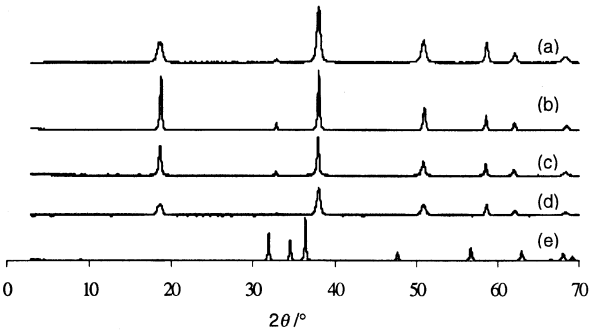

Fig. 1 Powder X-ray diffraction patterns for $Mg_{1-x}Zn_x(OH)_2$: (a) x = 0, (b) x = 0.1, (c) x = 0.25, (d) x = 0.5 and (e) x = 1 (ZnO).

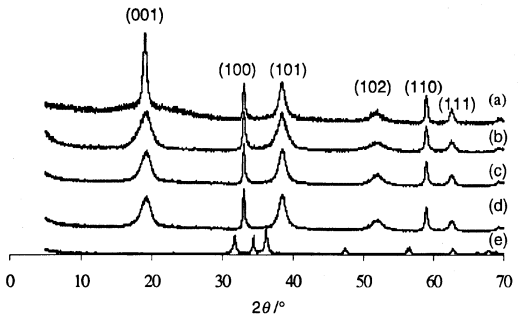

Fig. 2 Powder X-ray diffraction patterns for $Ni_{1-x}Zn_x(OH)_2$: (a) x = 0, (b) x = 0.1, (c) x = 0.25, (d) x = 0.5 and (e) x = 1 (ZnO).

Table 2 Lattice parameters for the mixed divalent magnesium–zinc hydroxides containing different Mg : Zn ratios

	Cell parameter/Å	
$Mg_{1-x}Zn_x(OH)_2$	$a = b$	c
x = 0	3.144	4.771
x = 0.1	3.145	4.761
x = 0.25	3.150	4.758
x = 0.5	3.151	4.747

Table 3 Lattice parameters for the mixed divalent nickel–zinc hydroxides containing different ratios Ni : Zn ratios

	Cell parameter/Å	
$Ni_{1-x}Zn_x(OH)_2$	$a = b$	c
x = 0	3.131	4.650
x = 0.1	3.131	4.650
x = 0.25	3.132	4.649
x = 0.5	3.144	4.630

The powder diffraction data show high crystallinity for the $Mg_{1-x}Zn_x(OH)_2$ series (Fig. 1) characterized by the sharp reflections. The patterns differ from the $Ni_{1-x}Zn_x(OH)_2$ series (Fig. 2), for which the reflections are broader except for the (100) and (110) reflections, due to the polymorphism in nickel hydroxide. Recently, Rajamashi *et al.*[39] reported the interstratification of β-$Ni(OH)_2$ with a low percentage of α motifs in the structure. This suggests that the isomorphous substitution of zinc into the interstratified β-nickel hydroxide also gives interstratified $Ni_{1-x}Zn_x(OH)_2$ materials.

The IR of series of both mixed divalent metal hydroxides are quite superimposable and are characterized by a sharp absorption at 3650 cm^{-1} due to non-hydrogen bonded hydroxy groups. Absorptions at 540 and 470 cm^{-1} are attributed to M–OH bending and M–O stretching vibrations. The spectra also exhibit a very broad absorption centred at *ca.* 3500 cm^{-1} indicative of hydrogen bonded hydroxy groups.

Mixed divalent metal phosphonate materials

Following reaction to form the mixed divalent metal phosphonates, the $Ni_{1-x}Zn_x(O_3PR)\cdot H_2O$ [with R = CH_3, C_2H_3, C_6H_5, $(CH_2)_2COOH$] are pale yellow powders in contrast to the green colour of the corresponding nickel–zinc hydroxide precursors. The $Mg_{1-x}Zn_x(O_3PR)\cdot H_2O$ materials [with R = CH_3, C_2H_3, C_6H_5] remain white.

The powder X-ray diffraction data for all the phosphonates prepared show high crystallinity and absence of any unreacted divalent metal hydroxides (Fig. 3). In Fig. 4, the series of X-ray patterns of $Mg_{1-x}Zn_x(O_3PCH_3)\cdot H_2O$ with different Mg : Zn ratios are given, demonstrating that for the whole series all products have the same structure. It should further be noted that even when we start with zinc oxide (x = 1) we obtain the same phosphonate phase as when using the hydroxide precursors. The interlayer spacing (defined as the perpendicular distance between the centres of the adjacent layers is related to the periodic spacing along the a axis) and can be determined from the (h00) reflections. $Mg_{1-x}Zn_x(O_3PR)\cdot H_2O$ and $Ni_{1-x}Zn_x(O_3PR)\cdot H_2O$ can be indexed on the basis of an orthorhombic unit cell, space group $Pmn2_1$ with cell parameters: b = 5.63–5.69, c = 4.77–4.86 Å for the Mg-containing phosphonates, and b = 5.55–5.69, c = 4.71–4.86 Å for those containing Ni. The a parameter varies according to the size of the organic group, R, from 8.71 to 8.75 Å for methyl from 14.31 to 14.43 Å for phenyl. We have also indexed new metal

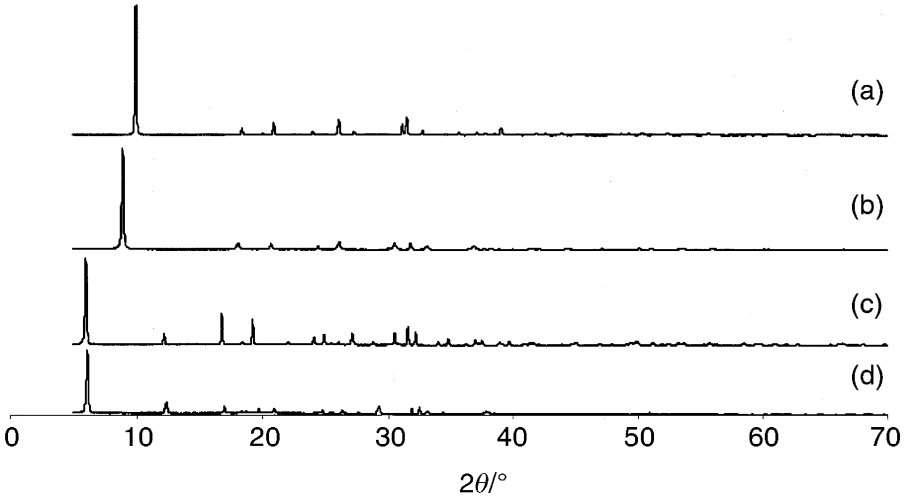

Fig. 3 Powder X-ray diffraction patterns for: (a) $Ni_{0.5}Zn_{0.5}(O_3PCH_3)\cdot H_2O$, (b) $Mg_{0.75}Zn_{0.25}(O_3PC_2H_3)\cdot H_2O$, (c) $Mg_{0.5}Zn_{0.5}(O_3PC_6H_5)\cdot H_2O$, (d) $Ni_{0.5}Zn_{0.5}(O_3P(CH_2)_2COOH)\cdot H_2O$.

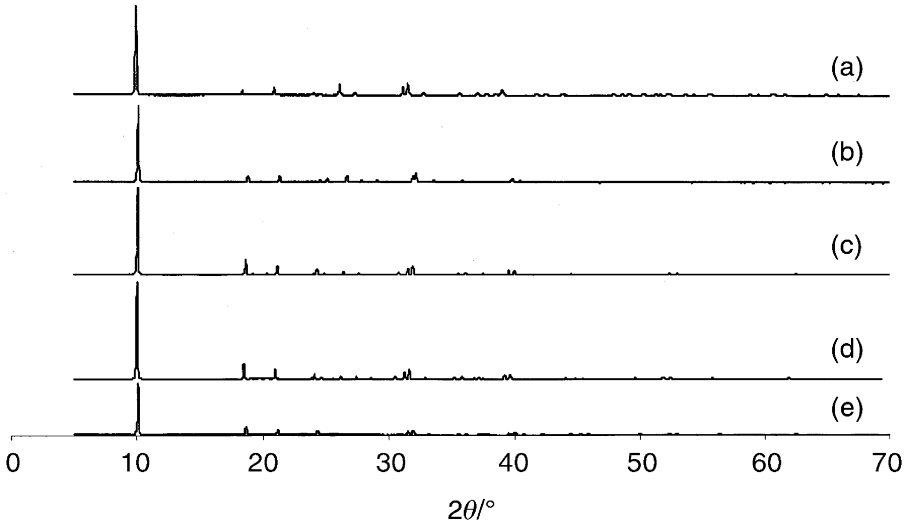

Fig. 4 Powder X-ray diffraction patterns for $Mg_{1-x}Zn_x(O_3PCH_3)\cdot H_2O$: (a) $x = 0$, (b) $x = 0.1$, (c) $x = 0.25$, (d) $x = 0.5$, (e) $x = 1$.

phosphonate materials: the mixed divalent metal vinylphosphonates $Mg_{1-x}Zn_x(O_3PC_2H_3)\cdot H_2O$ and $Ni_{1-x}Zn_x(O_3PC_2H_3)\cdot H_2O$ on the basis of the same orthorhombic space group, $Pmn2_1$, with $a = 9.81$–9.84 Å, which is as logically expected with the size of the vinyl group intermediate between that of methyl and phenyl.

Except for the end member zinc 2-carboxyethylphosphonate which has a different structure, the series $Ni_{1-x}Zn_x(O_3P(CH_2)_2COOH)\cdot H_2O$ has been also indexed (orthorhombic: space group $Pmn2_1$ with $a = 28.27$–28.48, $b = 5.60$, $c = 4.71$–4.73 Å) similar to that reported for the nickel 2-carboxyethylphosphonate in the literature.[38] [Note that the doubling of the a axis, as also observed in zirconium 2-carboxyethylphosphonate,[40] is due to a slight distortion in the structure induced by hydrogen bonding between the carboxylic acid groups]. The structure we obtain for these mixed Ni–Zn carboxyethylphosphonates suggests that neither nickel nor zinc are coordinated to the carboxylate groups, in contrast to the pure zinc 2-carboxyethylphosphonate (interlayer distance 9.43 Å) or copper 2-carboxyethylphosphonate[24] in which the metal is coordinated to the oxygens of the carboxylate group, rendering the material unable to undergo proton conduction.

In conclusion, the powder X-ray diffraction data for all the phosphonate materials prepared are consistent with the lamellar structure of $M^{II}(O_3PR)\cdot H_2O$ (M = Ni, Zn, Mn, Mg, Co, Cd) described previously in the literature,[7–9,13,38] and in which the metal cations are octahedrally coordinated.

The IR spectra (Fig. 5) of both $Mg_{1-x}Zn_x(O_3PR)\cdot H_2O$ and $Ni_{1-x}Zn_x(O_3PR)\cdot H_2O$ for the series of methyl-, vinyl-, phenyl- and 2-carboxyethyl-phosphonates show many similarities. The strong sharp bands around 3480 and 3420 cm^{-1} are attributed to stretching vibrations of the water molecule coordinated to the metal cations, while there is also a strong deformation around 1610 cm^{-1} attributed to the water molecule. In each case, bands in the 1150–980 cm^{-1} region are associated with the P–O vibrations of the PO_3 groups. For the methylphosphonates, two C–H stretching bands of the methyl group are seen at *ca.* 2995 and 2920 cm^{-1} (Fig. 5c), while for the vinylphosphonate materials bands in the 3120–2930 cm^{-1} region (Fig. 5b) correspond to the C–H stretch within the vinyl group. The aromatic C–H stretching bands (Fig. 5a) are located around 3050 and 3080 cm^{-1} for the different series of magnesium–zinc and nickel–zinc phenylphosphonates.

For the 2-carboxyethylphosphonates materials (Fig. 5d), the OH stretching vibrations of the water molecule coordinated to the metals are characterized by the bands around 3450 and 3430 cm^{-1} with a medium strength deformation band around 1637 cm^{-1}. The free OH from the carboxylic acid groups are associated with the broad band centred at 3400 cm^{-1}. The strong band at about 1695 cm^{-1} is attributed to the carbonyl group C=O, the frequency of which confirms that the oxygens

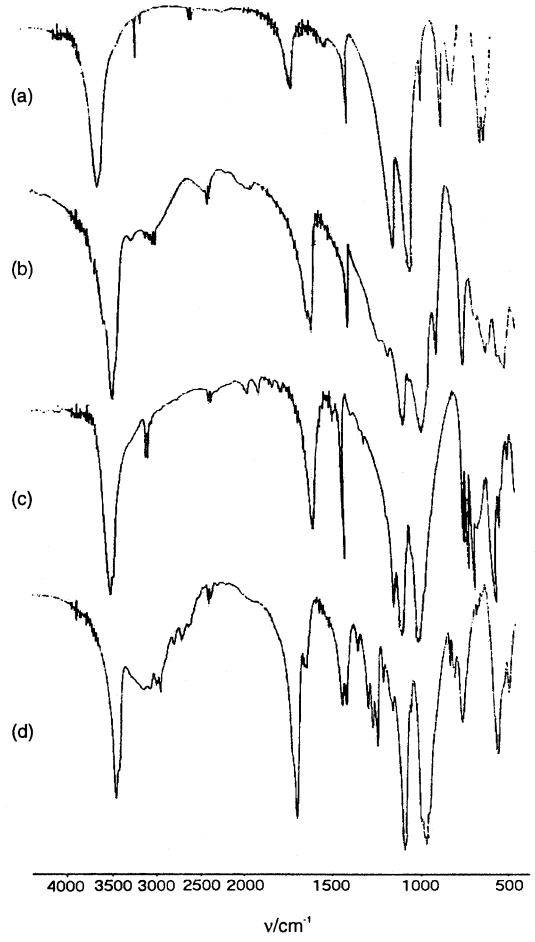

Fig. 5 FTIR spectra for: (a) $Ni_{0.5}Zn_{0.5}(O_3PCH_3)\cdot H_2O$, (b) $Mg_{0.75}Zn_{0.25}(O_3PC_2H_3)\cdot H_2O$, (c) $Mg_{0.5}Zn_{0.5}(O_3PC_6H_5)\cdot H_2O$, (d) $Ni_{0.5}Zn_{0.5}(O_3P(CH_2)_2COOH)\cdot H_2O$.

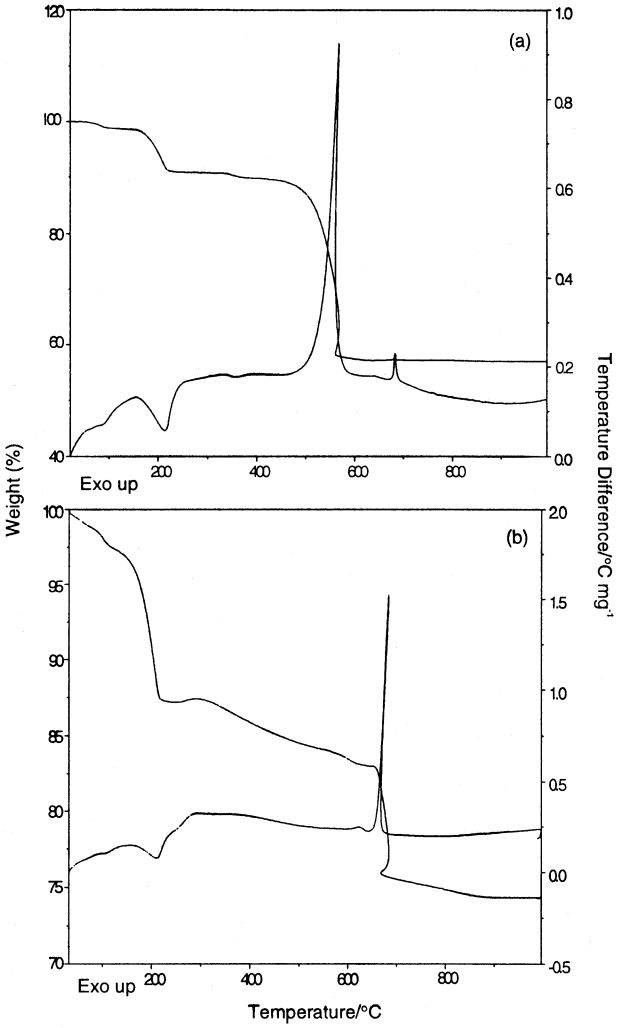

Fig. 6 TGA and DTA curves for: (a) $Mg_{0.5}Zn_{0.5}(O_3PC_6H_5)\cdot H_2O$, (b) $Mg_{0.5}Zn_{0.5}(O_3PC_2H_3)\cdot H_2O$.

of the carboxylic acid groups are free. Oxygens coordinated to the metals would be associated to a shift to lower frequency (1583 cm^{-1} in zinc 2-carboxyethylphosphonate).

The thermogravimetric curves for the magnesium–zinc and nickel–zinc methyl-, vinyl- and phenyl-phosphonates for all ranges of Mg : Zn and Ni : Zn ratios exhibit two stepwise mass losses. The first endothermic mass losses for the methyl and the phenyl compounds in the magnesium–zinc and nickel–zinc systems begins gradually about 100 °C and are attributed to the loss of the water molecule coordinated to the metals [TGA and DTA curves of $Mg_{0.5}Zn_{0.5}(O_3PC_6H_5)\cdot H_2O$ are shown in Fig. 6a]. The vinylphosphonate materials absorb the moisture from the air easier than the analogous phenyl or methyl materials and so the weight losses are less well defined (Fig. 6b). Dehydration begins at lower temperature (80 °C) with the removal of water adsorbed on the surface of the materials. For all the materials, the percentages weight losses are in agreement with those calculated theoretically, consistent with the removal of one molecule of water. There is also an exothermic mass loss around 520–550 °C for the magnesium–zinc and nickel–zinc methyl-, vinyl- and phenyl-phosphonates associated with oxidation of the organic component of the materials. A further small exothermic mass loss is observed between 680 and 720 °C, the final product of all the materials corresponds respectively to the mixed divalent magnesium–zinc and nickel–zinc pyrophosphates $(Mg_{1-x}Zn_x)_2P_2O_7$ and $(Ni_{1-x}Zn_x)_2P_2O_7$ characterized by X-ray powder diffraction and having similar patterns as $Mg_2P_2O_7$ and $Ni_2P_2O_7$ respectively. The theoretical percentage weight of the residues corresponds to those calculated for $1/2(Mg_{1-x}Zn_x)_2P_2O_7$ and for $1/2(Ni_{1-x}Zn_x)_2P_2O_7$ and IR provides further confirmation of the nature of these products with a strong band at 980 cm^{-1} attributed to P–O–P vibrations.

The thermogravimetric analysis of the $Ni_{1-x}Zn_x(O_3P(CH_2)_2COOH\cdot H_2O$ exhibits the same first stepwise mass loss as for the previous compounds with a first gradual mass loss which begins around 110 °C due to the removal of the water molecule within the coordination sphere of the metal. An extra endothermic mass loss occurs at 400 °C attributed to condensation of the carboxylic groups to form an anhydride, and the oxidation of the organic part of the materials is characterized by the exothermic mass loss about 540 °C. The residue has been identified, as above, as nickel–zinc pyrophosphate $(Ni_{1-x}Zn_x)_2P_2O_7$.

These thermogravimetric curves for the different phosphonates are again, as for the X-ray diffraction data, in good agreement with those of the structures containing one type of metal, further adding to the evidence that our mixed divalent metal phosphonates have the stoichiometries $Mg_{1-x}Zn_x(O_3PR)\cdot H_2O$ and $Ni_{1-x}Zn_x(O_3PR)\cdot H_2O$.

The range of $Mg_{1-x}Zn_x(O_3PCH_3)\cdot H_2O$ compounds have been also characterized by solid state ^{31}P MAS NMR (Fig. 7) to provide us structural information about the environment of the phosphorus atoms. The phosphorus resonance for pure zinc methylphosphonate monohydrate occurs at a different shift to that for the magnesium methylphosphonate monohydrate; the spectrum of $Zn(O_3PCH_3)\cdot H_2O$ contains a single sharp signal at $\delta = 34.36$ ppm while the $Mg(O_3PCH_3)\cdot H_2O$ contains one of approximately equal intensity at $\delta = 31.6$ ppm.

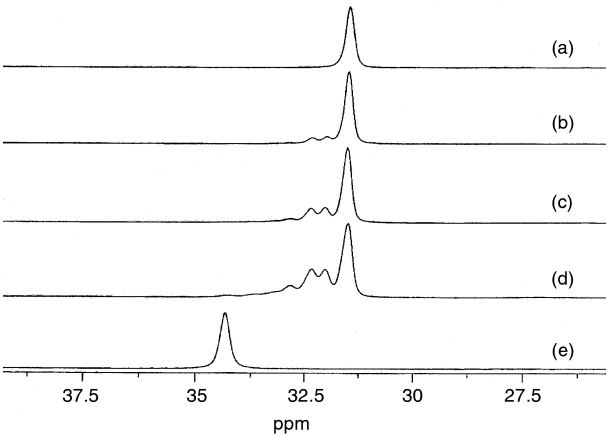

Fig. 7 Solid state ^{31}P MAS NMR spectrum of $Mg_{1-x}Zn_x(O_3PCH_3)\cdot H_2O$: (a) $x = 0$, (b) $x = 0.1$, (c) $x = 0.25$, (d) $x = 0.5$, (e) $x = 1$.

For the spectra of the mixed divalent magnesium–zinc methylphosphonate, we observe a distribution of small resonances between these two shifts. Indeed, for $Mg_{0.9}Zn_{0.1}(O_3PCH_3)\cdot H_2O$ we can easily see the main signal at $\delta = 31.6$ ppm, which is expected as the structure still predominantly contains Mg, but also two others discernible phosphorus resonances of lower intensity than the first at $\delta = 32.1$ and 32.4 ppm. The number and intensities of these signals increases with increasing Zn content in the structure, but at no stage do we see the presence of a phosphorus resonance corresponding to pure zinc methylphosphonate. For the $Mg_{0.75}Zn_{0.25}(O_3PCH_3)\cdot H_2O$ and $Mg_{0.5}Zn_{0.5}(O_3PCH_3)\cdot H_2O$, peaks are observed at $\delta = 31.6$, 32.1, 32.4 and 32.9 ppm. These observations confirm that we have different environments due to the presence of two different types of metal within the same structure. One possible interpretation, given that the peak of greatest intensity remains at $\delta = 31.6$ ppm for all Mg–Zn ratios, is that the Zn is not uniformly distributed throughout the structure but instead we have islands of mixed Mg–Zn phosphonate surrounded by 100% pure magnesium domains. In such a case, though, we would expect statistically as the Zn content increases to see equivalent domains of predominantly Zn phosphonate giving rise to a peak at $\delta = 34.36$ ppm. It is clear however that we do not have segregation into two different single phases of both pure magnesium and zinc methylphosphonate for which the sharp phosphorus resonance occurs at different shifts.

Conclusion

We have successfully derived a method by which we can obtain divalent metal phosphonate materials containing two different metals within the structure and having a layered structure similar to the analogous $M^{II}(O_3PR)\cdot H_2O$ phases. Synthesis of $Mg_{1-x}Zn_x(O_3PR)\cdot H_2O$ and $Ni_{1-x}Zn_x(O_3PR)\cdot H_2O$ by using the corresponding divalent metal hydroxides as precursors has been confirmed by the PXRD, IR, TGA and ^{31}P MAS NMR, clearly demonstrating that single phase materials have been formed. We are currently studying the intercalation of alkylamines into these materials, particularly into the magnesium–zinc phosphonates, as it is known that magnesium does not coordinate to amines while zinc does. Further mixed-divalent metal phosphonates are also under investigation, including systems containing copper in order to study the coordination of this metal into the structures.

Acknowledgement

We would like to acknowledge EPSRC for support (Research Grant to B. M.), and to thank Dr S. J. Kitchin for help in collecting the solid state NMR data.

References

1 A. Clearfield, in *Progress in Inorganic Chemistry*, ed. K. D. Karlin, Inc. John Wiley & Sons, New York, 1988, vol. 47.
2 A. Clearfield and J. A. Stynes, *J. Inorg. Nucl. Chem.*, 1964, **26**, 117.
3 A. Clearfield and G. D. Smith, *Inorg. Chem.*, 1969, **8**, 431.
4 J. M. Troup and A. Clearfield, *Inorg. Chem.*, 1977, **16**, 3311.
5 G. Alberti, M. Casciola, U. Costantino and R. Vivani, *Adv. Mater.*, 1996, **8**, 291.
6 A. Clearfield and U. Costantino, in *Comprehensive Supramolecular Chemistry*, ed. G. Alberti and T. Bein, Pergamon Press, Oxford, 1996, vol. 7, pp. 107–149.
7 G. Cao, H. Lee, V. M. Lynch and T. E. Mallouk, *Inorg. Chem.*, 1988, **27**, 2781.
8 G. Cao, H. Lee, V. M. Lynch and T. E. Mallouk, *Solid State Ionics*, 1988, **26**, 63.
9 K. J. Martin, P. J. Squattrito and A. Clearfield, *Inorg. Chim. Acta*, 1989, **155**, 7.
10 K. J. Frink, R.-C. Wang, J. L. Colon and A. Clearfield, *Inorg. Chem.*, 1991, **30**, 1438.
11 Y.-P. Zhang and A. Clearfield, *Inorg. Chem.*, 1992, **31**, 2821.
12 J. Lebideau, B. Bujoli, A. Jouanneaux, C. Payen, P. Palvadeau and J. Rouxel, *Inorg. Chem.*, 1993, **32**, 4617.
13 F. Fredoueil, D. Massiot, P. Janvier, F. Gingl, M. Bujoli-Doeuff, M. Evain, A. Clearfield and B. Bujoli, *Inorg. Chem.*, 1999, **38**, 1831.
14 A. Cabeza, M. A. G. Aranda, S. Bruque, D. M. Poojary and A. Clearfield, *Mater. Res. Bull.*, 1998, **33**, 1265.
15 L. Raki and C. Detellier, *Chem. Commun.*, 1996, 2475.
16 A. Cabeza, M. A. G. Aranda, S. Bruque, D. M. Poojary, A. Clearfield and J. Sanz, *Inorg. Chem.*, 1998, **37**, 4168.
17 P. Gerbier, C. Guerin, B. Henner and J.-R. Unal, *J. Mater. Chem.*, 1999, **9**, 2559.
18 D. M. Poojary, H. L. Hu, F. L. Campbell and A. Clearfield, *Acta Crystallogr. Sect B*, 1993, **49**, 996.
19 D. Cunningham, P. J. D. Hennelly and T. Deeney, *Inorg. Chim. Acta*, 1979, **37**, 95.
20 S. Drumel, P. Janvier, D. Deniaud and B. Bujoli, *J. Chem. Soc., Chem. Commun.*, 1995, 1051.
21 S. Drumel, P. Janvier, P. Barboux, M. Bujoli-Doeuff and B. Bujoli, *Inorg. Chem*, 1995, **34**, 148.
22 S. J. Hartman, E. Todorov, C. Cruz and S. C. Sevov, *Chem. Commun.*, 2000, 1213.
23 A. Clearfield, *Chem. Mater.*, 1998, **10**, 2801.
24 G. B. Hix, B. M. Kariuki, S. Kitchin and M. Tremayne, *Inorg. Chem.*, 2001, **40**, 1477.
25 C.-Y. Yang and A. Clearfield, *React. Polym.*, 1987, **5**, 13.
26 G. Alberti, M. Casciola, U. Costantino, A. Peraio and E. Montoneri, *Solid State Ionics*, 1992, **50**, 315.
27 G. Alberti, M. Casciola, R. Palombari and A. Peraio, *Solid State Ionics*, 1992, **58**, 339.
28 G. Alberti and M. Casciola, *Solid State Ionics*, 1997, **97**, 177.
29 E. Jaimez, G. B. Hix and R. T. C. Slade, *Solid State Ionics*, 1997, **97**, 195.
30 P. M. D. Giaccomo and M. B. Dines, *Polyhedron*, 1982, **1**, 61.
31 G. Cao and T. E. Mallouk, *Inorg. Chem.*, 1991, **30**, 1434.
32 Y.-P. Zhang, K. J. Scott and A. Clearfield, *Chem. Mater.*, 1993, **5**, 495.
33 Y.-P. Zhang, K. J. Scott and A. Clearfield, *J. Mater. Chem.*, 1995, **5**, 315.
34 D. M. Poojary and A. Clearfield, *J. Am. Chem. Soc.*, 1995, **117**, 11278.
35 S. Drumel, P. Janvier, M. Bujoli-Doeuff and B. Bujoli, *J. Mater. Chem.*, 1996, **6**, 1843.
36 M. Bujoli-Doeuff, M. Evain, P.-A. Jaffres, V. Caignaert and B. Bujoli, *Int. J. Inorg. Mater.*, 2000, **2**, 557.
37 S. Drumel, M. Bujoli-Doeuff, P. Janvier and B. Bujoli, *New J. Chem.*, 1995, **19**, 239.
38 G. B. Hix and K. D. M. Harris, *J. Mater. Chem.*, 1998, **8**, 579.
39 M. Rajamathi, P. V. Kamath and R. Seshadri, *J. Mater. Chem.*, 2000, **10**, 503.
40 G. Alberti, U. Costantino, M. Casciola, R. Vivani and A. Peraio, *Solid State Ionics*, 1991, **46**, 61.